Analysis of Pyramidal Microwave Absorbers for Enhanced Performance in 1 – 10 GHz Frequency Range

Aya Raad Thanoon and Khalil H. Sayidmarie

Ninevah University, Mosul, Iraq

https://doi.org/10.26636/jtit.2025.2.2092

Abstract — One of the main applications of microwave absorbers is in anechoic chambers, where the walls are lined with pyramidal foam impregnated with a lossy material. This paper investigates the impact that various design parameters of pyramidal microwave absorbers exert on their performance, with the aim of finding the best design values that ensure better operational properties. Typical pyramid absorbers were investigated by conducting simulations with the use of the CST Microwave Suite simulator, across the frequency range of 1 – 10 GHz, at various angles of the incident wave. The investigations also considered absorbers backed by conducting plates that are used in shielded anechoic chambers. The study shows that higher permittivity leads to higher reflection, while increased loss tangent improves absorption, and the same applies to magnetic materials. Larger pyramid heights lead to lower reflection, but only in the case of thicker absorbers. A pyramidal absorber with the height of 16 cm, designed using lossy material with permittivity and permeability of 1.5 and loss tangent of 0.5 achieved a reflection coefficient that was lower than –60 dB for frequencies between 3 and 10 GHz. The results are useful in designing absorbers relying on materials that offer only dielectric or magnetic properties, or that combine both of them to achieve enhanced performance.

Keywords — anechoic chambers, dielectric loss, microwave absorber, reflectivity

1. Introduction

Microwave absorbers are commonly used in many applications, such as radar, military defense systems, and compliance testing of electronic devices. Their primary aim is to reduce or eliminate the reflection, transmission, and scattering of microwave radiation, thereby minimizing interference or reducing the risk of detection in many sensitive applications.

However, newly built RF and microwave devices and systems must be experimentally tested to assess their performance and evaluate their radiation leakage. Testing of these devices must be conducted either in an open area that is free of any surrounding objects and other interference generating devices, or inside an anechoic chamber. The former solution is rather expensive and may not always be available due to weather conditions, while anechoic chambers are readily available.

Currently, commercially available absorbers are mostly constructed of polyurethane and polystyrene foam impregnated with materials that absorb electromagnetic energy. Many of these absorbers use carbon or its derivatives as a lossy material. Other types rely on ferrites, polymers, and lossy dielectric materials [1].

The efforts to improve the performance of microwave absorbers can be divided into the following stages:

- selecting a suitable and cheap lossy material,
- choosing a proper profile of the absorber's surface and its thickness,
- determining the frequency range across which acceptable reflection levels are achieved,
- deciding on the weight of the absorber.

Certain agricultural leftovers, such as coconut shells, banana peels, sugar cane, water hyacinth, and other byproducts have been suggested as alternatives to foam in absorber construction. The author of [2] mixed rubber tire dust and rice husk in three different ratios (50:50, 25:75, and 75:25) to build a microwave absorber. For a 15 cm thick absorber, the average reflection coefficient obtained equaled –22.03 dB, –21.54 dB, and –32.51 dB, respectively, in the frequency range of 7 to 13 GHz.

In [3], sugar cane bagasse was used to build pyramidal microwave absorbers operating in the frequency range of 0.1 – 20 GHz, with an average reflection of –44 dB. The authors of [4] used rice husk and a mixture of rice husk and coal to construct pyramid microwave absorbent structures which produced mean reflections of –30 dB and –40 dB, respectively. Furthermore, the authors of [5] proposed the use of water hyacinth to fabricate microwave absorbers, achieving reflectivity values ranging from –30 to –10 dB for a 13 cm thick absorber. In [6], a mixture of two materials, such as polyurethane and carbon, was proposed for use in the frequency range of 1 – 10 GHz. The fabricated absorber, being 30 cm thick, achieved a reflection coefficient of –30 dB at 3 GHz.

The shape of the absorber is another important factor in determining the level of the reflection, since it forms the boundary between the air and the lossy material of the absorber where the electromagnetic wave is incident. At this interface, the law of reflection is derived by applying the boundary conditions. Pyramidal absorbers were extensively used, as they usually offer a smooth and gradual change from the air to the absorbing material. The performance of pyramidal and truncated

pyramidal absorbers with relative permittivity values of 2.5, 2.9 and 3.3, made of solid, hollow or coated materials were investigated in [7]. The collected data, which were presented as the best or average values, demonstrated that slightly higher permittivity corresponded to somewhat higher reflection. This is because as the absorber's permittivity increases along with the increase in the reflection of the incident wave from its surface.

In [8], a triangular pyramid, an isosceles pyramid, and an equilateral pyramid were investigated, with rice husks as the absorbing medium, at frequencies of 1 – 20 GHz, and the results obtained results showed that the shape of the pyramid base could affect the performance of the entire absorber. Paper [9] examined a hexagonal pyramid made from banana leaves, rice husks, and rice straws, at frequencies ranging from 0.01 to 20 GHz. The results obtained for 13 cm thick absorbers showed reflection levels of –35 dB, –39 dB, and –38 dB, respectively. The same agricultural residues were also applied to truncated hexagonal pyramids which offered lower reflection coefficients of –35 dB, –35 dB, and –37 dB, respectively.

Another shape, such as wall tiles made of kenaf and coconut coir was investigated in [10] as an absorber for the frequency range of 1 to 12 GHz. The kenaf had the highest absorption in the C band and the coconut coir showed better results in the X band. In [11], carbon from biomaterials was used and its reflectance was typically lower than –25 dB.

Although the pyramidal shape offers a gradual introduction of the absorbing material, planar multilayer microwave absorbers have also been employed. Their configuration comprises several layers (all characterized by different thicknesses) of various types of materials that differ in terms of their electrical and magnetic properties. Such a solution is effective in multiple frequency bands and offers better performance provided it is well optimized at the design stage [12].

Metamaterial surfaces can be designed to work as electromagnetic wave absorbers characterized by decent efficiency, and their geometric structures may be used to improve the performance of traditional absorbers. A metamaterial absorber with three layers of different resistive films and a central via was presented in [13]. A 90% absorption rate was obtained across the frequency range of 3.2 to 35.5 GHz or 167% relative bandwidth. However, the level of the reflection coefficient was not provided, as the emphasis was placed on bandwidth and absorption. In [14], lossy carbon paint was applied to a frequency-selective surface (FSS) to enhance the absorption rate. While this absorber is very thin, the bandwidth achieved was limited.

Hollow pyramidal absorbers (HPA) can offer an additional degree of freedom in optimizing broadband performance by furnishing hollow sections of various sizes. Thus, they can absorb waves within a wider range of frequencies. The authors of [15] designed a slotted HPA that contains slots of isosceles triangles, which achieved absorptivity of –26.32 dB, in the L, S, C, and X frequency bands. [16] introduced a triangular-slotted HPA using the Sierpinski principle. The conclusion was that an increase in the number of smaller slots resulted in the highest level of absorption, the most stable impedance, and the widest bandwidth.

The former studies focused on the suitability of certain materials, with less emphasis placed on the preferred characteristics of the material that are required in order to ensure better performance. Moreover, the pyramidal shape was extensively used, but the dimensions that yield the lowest reflection remained unclear.

This study explores the performance of the pyramid absorber and the impact that its height, base size, permittivity, permeability, $\tan\delta$, and angle of incidence exert on the electromagnetic wave (EM) applied. The aim is to find a combination of dimensions and material properties capable of achieving better performance. Furthermore, it investigates the case where the absorber is backed by a conducting plate that is employed in shielded anechoic chambers.

The paper is organized as follows. Section 2 analyzes the reflection of the EM wave from lossy dielectric surfaces. Section 3 presents the modeling of the pyramidal absorber using CST software, while Section 4 explores the effect of the various absorber parameters. Section 5 investigated the case of absorbers supported by a conducting plate, while Section 6 contains considerations on the type of plane surface material. Section 7 provides a comparison with other published works. The conclusions drawn are presented in Section 8.

2. Analysis of Reflection at the Air-dielectric Boundary

The impact that microwave absorbers exert on incident EM waves depends on the reflection coefficient, properties of the dielectric material of the absorber and its geometry. Dielectric and magnetic properties of the absorber are important factors determining absorption performance. The relative complex permittivity is typically written as:

$$\varepsilon_r = \varepsilon_r' - j\varepsilon_r'' \,, \tag{1}$$

where ε_r' represents the material's energy storage capacity and ε_r'' indicates the losses suffered due to the electric field. The electric loss tangent is the ratio between the imaginary and real parts of permittivity, and is expressed as:

$$\tan\delta_d = \frac{\varepsilon_r''}{\varepsilon_r'} \,. \tag{2}$$

Similarly, the relative permeability of the complex is:

$$\mu_r = \mu_r' - j\mu_r'' \,, \tag{3}$$

where μ_r' represents the material's ability to store magnetic energy and μ_r'' indicates the losses suffered due to the magnetic field. The magnetic loss tangent is the ratio between the imaginary and real parts of permeability, and is expressed as:

$$\tan\delta_m = \frac{\mu_r''}{\mu_r'} \,. \tag{4}$$

The three basic scenarios for the reflection of an EM wave that arrives at a specific material from the air are shown in Fig. 1. The reflection coefficient for a normally incident wave

on a planar medium can be given by [17]:

$$\Gamma = \frac{\eta - \eta_0}{\eta + \eta_0}\,, \tag{5}$$

where:

$$\eta_0 = \sqrt{\frac{\mu_0}{\varepsilon_0}} \text{ and } \eta = \sqrt{\frac{j\omega\mu}{\sigma + j\omega\varepsilon}}$$

are the intrinsic impedances of air and the absorber material, respectively. By substituting these in Eq. (5), it can be shown that for a general material, the reflection coefficient can be written as:

$$\Gamma = \frac{1 - \sqrt{\frac{\varepsilon_r}{\mu_r} - \frac{j\sigma}{\omega\varepsilon_0\mu_r}}}{1 + \sqrt{\frac{\varepsilon_r}{\mu_r} - \frac{j\sigma}{\omega\varepsilon_0\mu_r}}}\,, \tag{6}$$

which for lossless material ($\sigma = 0$) reduces to:

$$\Gamma = \frac{1 - \sqrt{\frac{\varepsilon_r}{\mu_r}}}{1 + \sqrt{\frac{\varepsilon_r}{\mu_r}}}\,, \tag{7}$$

where ε_r and μ_r are the relative complex dielectric constant of the complex and the relative permeability of the complex given by Eq. (1) and Eq. (3), respectively. After substitution for ε_r and using Eq. (2), the reflection coefficient for a nonmagnetic material Γ can be expressed using two forms:

$$\Gamma = \frac{1 - \sqrt{\varepsilon_r' - j\varepsilon_r''}}{1 + \sqrt{\varepsilon_r' - j\varepsilon_r''}}\,, \tag{8}$$

$$\Gamma = \frac{1 - \sqrt{\varepsilon_r'}\sqrt{1 - j\tan\delta_d}}{1 + \sqrt{\varepsilon_r'}\sqrt{1 - j\tan\delta_d}}\,. \tag{9}$$

For the absorber limiting case when the dielectric material of the absorber is lossless ($\varepsilon_r'' = 0$, or $\tan\delta_d = 0$), Eq. (8) and (9) will be:

$$\Gamma = \frac{1 - \sqrt{\varepsilon_r'}}{1 + \sqrt{\varepsilon_r'}}\,. \tag{10}$$

Equation (10) indicates that a higher relative permittivity ε_r' leads to larger reflection values, while Eq. (9) indicates that a higher value of the loss tangent $\tan\delta_d$ also leads to higher reflection.

Similarly, it can be shown that the reflection coefficient for an absorber made of magnetic material with $\varepsilon_r = 1$, and $\tan\delta_d = 0$ is:

$$\Gamma = \frac{\sqrt{\mu_r' - j\mu_r''} - 1}{\sqrt{\mu_r' - j\mu_r''} + 1}, \tag{11}$$

For the limiting case where the magnetic material of the absorber is lossless, $\mu_r'' = 0$, or $\tan\delta_m = 0$, Eq. (11) will be:

$$\Gamma = \frac{\sqrt{\mu_r'} - 1}{\sqrt{\mu_r'} + 1}\,. \tag{12}$$

Equations (11), (12) indicate that higher relative permeability μ_r' leads to larger reflection values. Higher value of the loss tangent $\tan\delta_m$ also leads to increased reflection.

The above relations have been derived for a plane air-dielectric interface. Thus, they cannot be applied directly to the pyramidal shape of the absorber, but offer a clear insight into the reflection generated by the absorber. Moreover, Eq. (7) shows that for a loss-free material, when the relative dielectric constant approaches the relative permeability, the reflection coefficient trends towards zero.

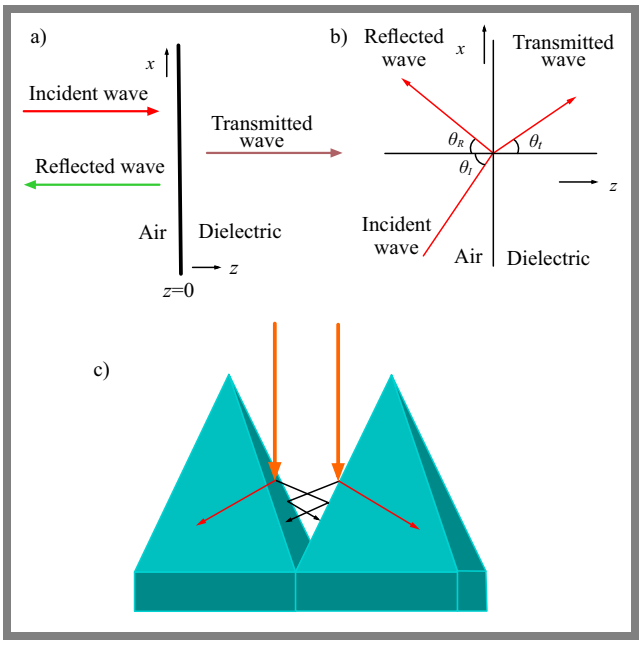

Fig. 1. Basic scenario for the reflection of an EM wave from a dielectric surface: a) normal incidence, b) oblique incidence, and c) incidence on the surface of a pyramidal absorber.

When the EM wave is incident obliquely on the dielectric material, then the reflection coefficient will be influenced by the angle of incidence and polarization with respect to the interface. The reflection coefficient for parallel $\Gamma_{\parallel}$ and perpendicular $\Gamma_{\perp}$ polarization is given, respectively, by [17]:

$$\Gamma_{\parallel} = \frac{\eta\cos\theta_t - \eta_0\cos\theta_i}{\eta\cos\theta_t + \eta_0\cos\theta_i}\,, \tag{13}$$

$$\Gamma_{\perp} = \frac{\eta\cos\theta_i - \eta_0\cos\theta_t}{\eta\cos\theta_i + \eta_0\cos\theta_t}\,, \tag{14}$$

The angle of incidence θ_i is another influencing factor. When a pyramidal absorber is considered, oblique incidence is inevitable, even if the wave is normally incident on the absorber, as seen in Fig. 1c. Moreover, the wave may reflect from one pyramid's surface towards an adjacent pyramid. Such a case is difficult to analyze using the ray approach, and therefore the use of CST simulation can be a powerful technique to evaluate the reflection's properties.

3. Analysis of a Pyramidal Microwave Absorber

Figure 2 shows the construction of a pyramidal microwave absorber that was modeled using the CST simulator. The pyramidal shape was chosen by many designers and manufacturing companies since it offers a gradual change from the air to the absorbing material. Moreover, the sides of neighboring pyramids generate multiple reflections, with a fraction of the incident wave's power being absorbed in each reflection.

Computer simulations assumed a typical pyramidal absorber with a base of 10 × 10 cm with a thickness of 5 cm, and

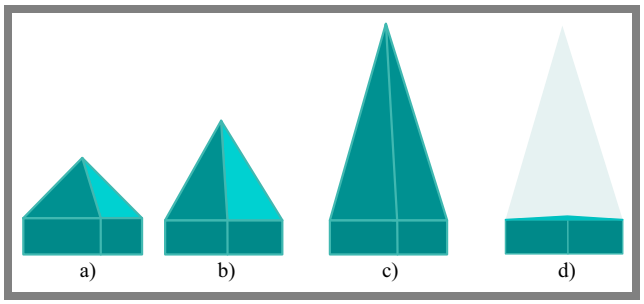

Fig. 2. Investigated pyramidal microwave absorber with heights of: a) 8 cm b) 16 cm, and c) 24 cm. The base of the pyramid is shown in d).

pyramid height values of 8 cm, 16 cm, and 24 cm. Various relative permittivity and loss tangent values were selected as parameters in the simulation.

4. Results of the Simulations

The pyramidal absorber was modeled using the unit cell approach with two ports, as shown in Fig. 3. The EM wave was incident on port 1, and the reflection coefficient $S_{11}$was determined at port 1, while the transmission coefficient S_{21} was determined at port 2. The unit cell approach was adopted in the modeling of the absorber, and the frequency domain solver was employed in the calculations.

The influence of the various absorber parameters, such as relative permittivity, relative permeability, loss tangent, pyramid height, and angle of the incident wave, were studied by a parameter sweep. In these investigations, one of the parameters was varied, while the remaining variables remained fixed, and the obtained results were used to draw conclusions concerning the impact the variable parameter exerted on the absorber's performance. The results obtained are presented and discussed in the following subsections.

4.1. Effect of Relative Permittivity

Relative permittivity of the absorber material is an important factor in determining the reflection coefficient. The reflection coefficient for an EM wave propagating from the air onto a plane dielectric material was discussed in Section 2. While that section offered a basic idea about the reflection mechanism, a closed-form relation is difficult to derive for the pyramidal case. Thus, the investigation using CST modelling is capable of offering a faster and easier insight into the investigation.

Figure 4 shows the variation of the reflection coefficient of a non-magnetic absorber with frequency for three values of relative permittivity (1.5, 2.5, and 3.5), with the loss tangent fixed at 0.5, and the height of the pyramid set at 16 cm. The results show that for frequencies above approximately 5 GHz, the reflection increases along with relative permittivity, as indicated by Eq. (10), for the plane dielectric material. However, this trend is not evident at lower frequencies.

This finding may be attributed to the fact that for frequencies above 5 GHz, where the wavelength in the air is smaller

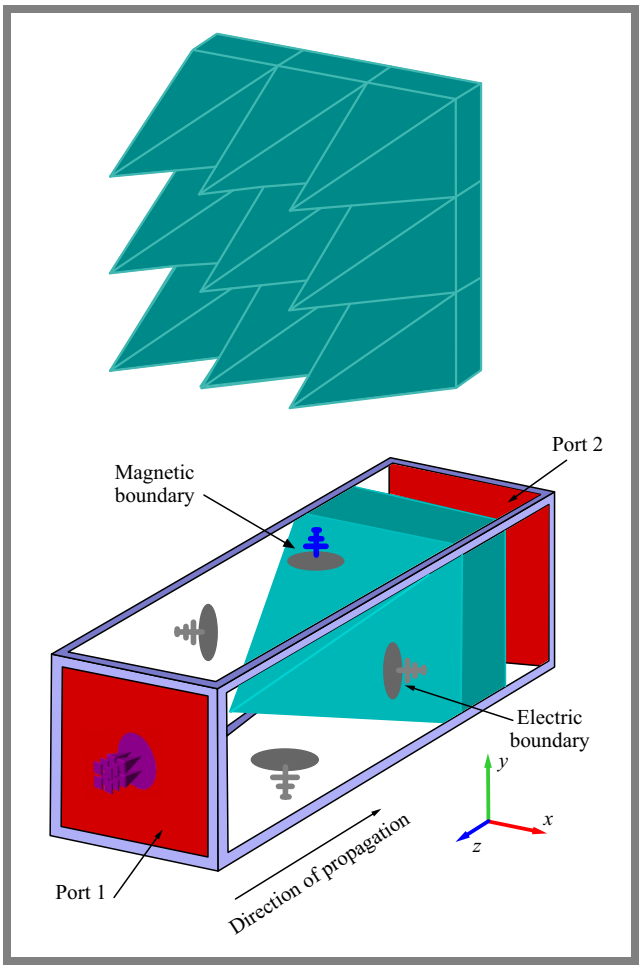

Fig. 3. Simulation model used in the CST Microwave software.

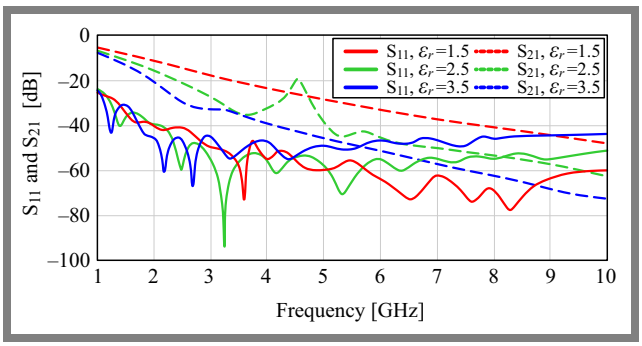

Fig. 4. Variation of the reflection coefficient $|S_{11}|$ and transmission coefficient $|S_{21}|$ with frequency for pyramid height of 16 cm and $\tan\delta_d$, with various values of ε_r.

than 6 cm, behavior of the absorber's surface is closer to that of a plane dielectric layer. However, for lower frequencies, the absorber size is comparable to the wavelength, and the approximation of the absorber by a plane surface departs from the actual case. The variation of the reflection coefficient with frequency shows a faster decline at lower frequencies, compared to a scenario involving higher frequencies.

The same figure illustrates the variation of the transmission coefficient $|S_{21}|$ with changes in frequency, indicating decreasing values at higher frequencies. Moreover, as the reflection increases with increasing relative permittivity, less power

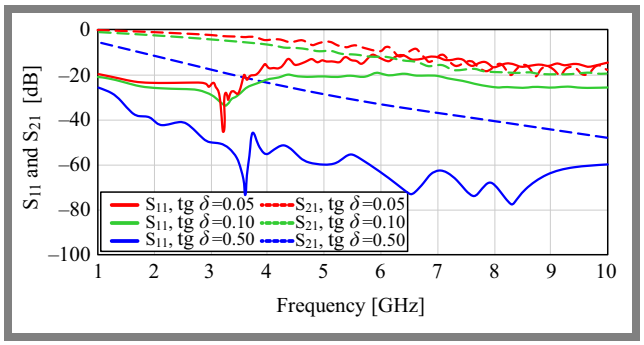

Fig. 5. Variations of reflection coefficient $|S_{11}|$ and transmission coefficient $|S_{21}|$ along with frequency changes, for pyramid height of 16 cm and $\varepsilon_r = 1.5$, for various values of $\tan\delta_d$.

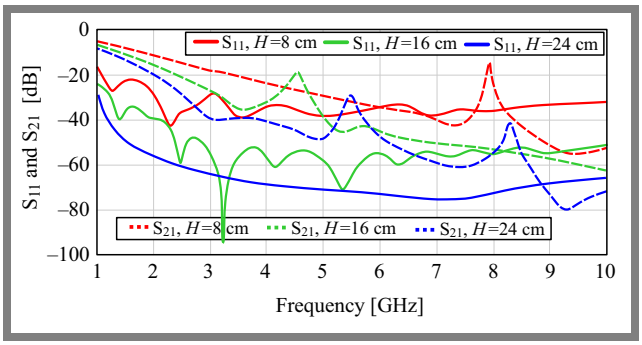

Fig. 6. Variation of reflection coefficient $|S_{11}|$ and transmission coefficient $|S_{21}|$ along with frequency changes, for pyramid heights of 8, 16, and 24 cm, for $\varepsilon_r = 2.5$ and $\tan\delta_d = 0.5$.

is introduced into the absorber, leading to lower transmitted power.

4.2. Effect of Loss Tangent

The loss tangent $\tan\delta_d$ of the absorber material is an important factor in absorbing the EM wave that penetrates into the absorber material, as it influences the level of the reflected wave that leaves the absorber. Figure 5 shows the level of the reflection coefficient for a non-magnetic material having $\tan\delta_d$ values of 0.05, 0.1, and 0.5, while the pyramid height was kept at 16 cm, and $\varepsilon_r = 1.5$. One may clearly see those higher values of loss tangent $\tan\delta_d$ lead to lower reflection levels. The effect is more pronounced at higher frequencies.

An increase in the loss tangent indicates an increase in the material's ability to convert electromagnetic waves into heat, hence reducing the reflected energy. This explains why the reflection coefficient decreases as the loss tangent increases. On the other hand, as the loss tangent increased, the transmission coefficient S_{21} decreased, as the wave penetrating the absorber experienced more losses.

4.3. Effect of Pyramid Height

The height of the pyramid is a determinant factor in specifying the thickness of the absorber, and thus the total volume of the absorbing material and the overall shape of the absorber. For a fixed base size, a larger height of the pyramid means a narrower tip and consequently smoother introduction of the absorber material into the air, which will lead to reduced reflection. However, a larger height means a thicker absorber, thus resulting in more weight and cost.

Figure 6 shows the effect of pyramid height H on the achieved reflection of the absorber, where H was varied from 8 to 16 cm, and 24 cm, with the parameters of the non-magnetic material remaining fixed at $\varepsilon_r = 2.5$, $\tan\delta_d = 0.5$.

The results obtained show that a larger pyramid height leads to a lower reflection. An average improvement of approximately 20 dB in the reflection coefficient is noticed when the height increases from 8 to 16 cm, while an improvement between 15 to 20 dB can be noticed when the height is further increased to 24 cm. This finding can be explained by the fact that a larger height, with fixed base dimensions, means larger

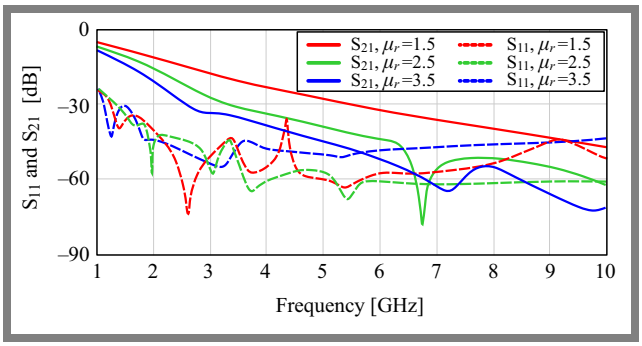

Fig. 7. Variation of reflection coefficient $|S_{11}|$ and transmission coefficient $|S_{21}|$ along with frequency changes, for pyramid height 16 cm and $\tan\delta_m = 0.1$, with various values of μ_r, $\varepsilon_r = 1$ and $\tan\delta_d = 0$.

absorbing volume and thus more losses and, consequently, a lower reflection.

Moreover, a larger height at a fixed base means a smaller tip angle of the pyramid. This results in a more gradual introduction of the absorber material and, consequently, a lower reflection.

Figure 6 also shows the variation of the transmission coefficient $|S_{21}|$ with frequency for various heights of the pyramid. It is noted that larger heights lead to lower transmission, since the loss caused by the absorber is proportional to its thickness.

4.4. Effect of Permeability

The permeability of the absorber material also affects its performance as it influences both the reflection and absorption inside the material due to the imaginary part of μ. Figure 7 illustrates the performance of the investigated absorber when only the magnetic properties are considered, while the dielectric properties are excluded ($\varepsilon_r = 1$, $\tan\delta_d = 0$).

One may notice that both reflection and transmission coefficients decrease along with the increase in frequency. Furthermore, each of the coefficients increases as the relative permeability μ_r is increased. The general trend of the variation is similar to that illustrated in Fig. 4, when relative permittivity was varied for a non-magnetic material. The similarity in the behavior can be understood by comparing Eq. (10) with Eq. (12), indicating similar relations between re-

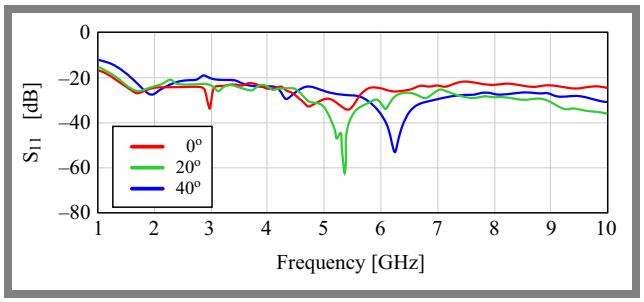

Fig. 8. Variation of reflection coefficient $|S_{11}|$ with frequency changes, for pyramid height of 8 cm, $\varepsilon_r = 1.5$ and $\tan\delta_d = 0.1$, at various incidence angles of $0°$, $20°$, $40°$.

flection coefficient Γ and the real parts of permittivity and permeability, respectively.

Further simulations performed to evaluate the effect of the loss tangent and pyramid's height generated similar results to those shown in Figs. 5, 6, respectively and the results are not presented here for brevity.

4.5. Effect of Angle of Incidence

In the cases investigated in the previous sections, the EM wave was normally incident on the absorber. However, oblique incidence at a specific angle is encountered in the majority of scenarios. The impact of the angle of incidence stems from the fact that the reflection coefficient depends on the incidence angle with respect to the absorber's surface and the properties of the absorber's material.

The relations of Eqs. (13) and (14) show the effect that the angle of incidence and the absorber's parameters have on the reflection coefficient when the EM wave is incident on a half-plane dielectric material. However, closed-form relations for pyramidal absorbers will be very difficult to derive. The effect of the angle of incidence was investigated using proper settings introduced to the CST software.

Figure 8 shows the effect of changing the angle of incidence on a non-magnetic pyramid absorber while fixing the other parameters height of 8 cm, $\varepsilon_r = 1.5$, and $\tan\delta_d = 0.1$. The variation in the reflection coefficient is approximately 10 dB for angles ranging from $0°$ to $40°$. Moreover, lower variations may be observed at lower frequencies. For the case of inclined incidence, the EM wave will face the pyramid's surface and may penetrate the absorber, exiting from the other side and thus contributing to the reflected wave.

5. Reflection from Conductor-backed Absorbers

Many echoic chambers are also designed to shield EM waves. In these designs, the walls of the chamber are usually covered by conducting sheets and then the absorbers are placed on the conducting walls. These designs can be modeled by placing a conducting plane underneath the absorber.

The CST Microwave Suite was used in the modeling process, with a 1 mm thick copper sheet placed under the pyramidal absorber, as shown in Fig. 9. The results obtained for such

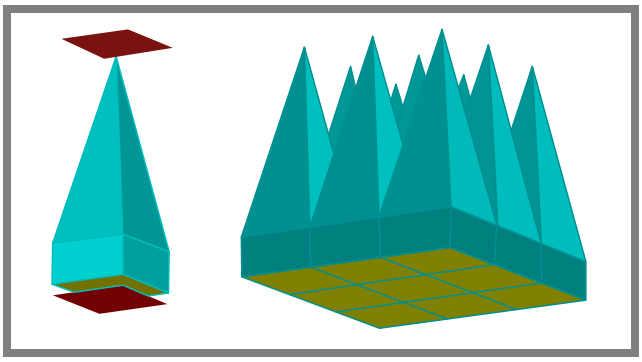

Fig. 9. Model simulated using the CST Microwave Suite with a copper sheet placed below the pyramidal absorber.

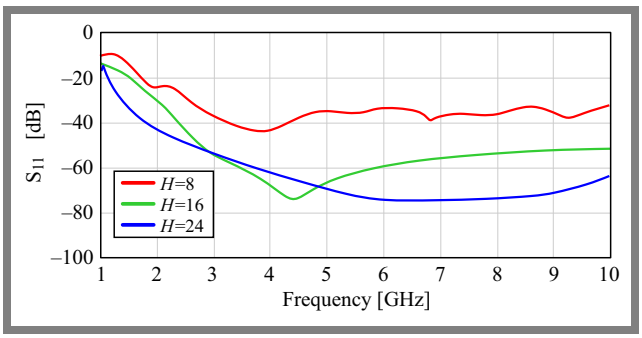

Fig. 10. Variation of reflection coefficient $|S_{11}|$ with frequency changes for a pyramidal absorber backed by a 1 mm thick copper plate, where $\varepsilon_r = 2.5$, $\tan\delta_d = 0.5$, for $H = 8$, 16, and 24 cm.

a setup are shown in Fig. 10 for a normal incident wave. The reflection coefficient decreases as the thickness of the absorber increases from 8 to 16 cm and then to 24 cm.

A thicker absorber means that the incident wave propagates through the absorbing material towards the back conductor, where it is fully reflected, and then travels back towards the direction of incidence. This means the wave is attenuated twice inside the absorber. Thus, for adequate losses in the absorber material, the reflected wave is mainly that was initially reflected at the absorber surface.

To show the effect of the back conducting plane, Fig. 11 compares the results obtained for three various backplanes: a 35 µm thick copper plate, a 1 mm copper plate, and a 1 mm galvanized iron plate. The results show similar performance except for the frequency range of 2.5 to 5.5 GHz. The iron plate has shown a reflection of less than –50 dB across 75% of the frequency range and can be considered the best choice in terms of cost and performance.

6. Electric and Magnetic Properties

Investigations described in the previous sections have shown that lossy dielectric and magnetic materials can be used to design microwave absorbers. The employment of a material having both properties will increase the absorption rate and may help reduce the reflection from the absorber.

As estimated by Eq. (7), the reflection from a plane surface of a certain material can be reduced if the relative values of its permittivity and permeability are equal.

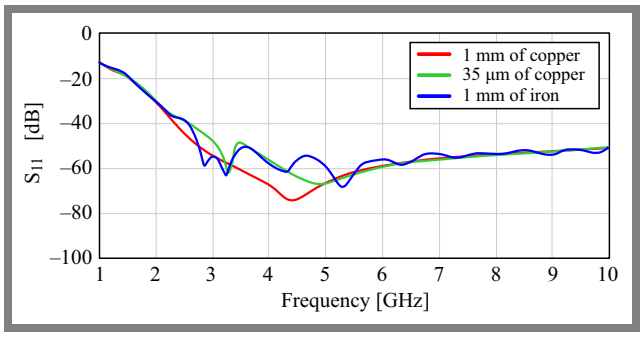

Fig. 11. Variation of reflection coefficient $|S_{11}|$ along with frequency changes for a pyramidal absorber with the height of 16 cm, $\varepsilon_r = 2.5$ and $\tan\delta_d = 0.5$, with the following back plate options: 35 µm copper, 1 mm copper, and 1 mm iron.

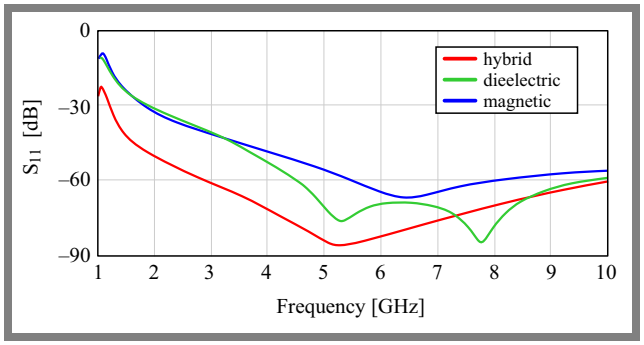

Fig. 12. Changes in reflection coefficient $|S_{11}|$ along with frequency changes for a 16 cm tall pyramidal absorber and a 1 mm iron backing plate for three scenarios: a) $\varepsilon_r = \mu_r = 1.5$ and $\tan\delta_d = \tan\delta_m = 0.5$, b) $\varepsilon_r = 1.5$, $\tan\delta_d = 0.5$, $\mu_r = 1$, and $\tan\delta_m = 0$, c) $\mu_r = 1.5$, $\tan\delta_m = 0.5$, $\varepsilon_r = 1$, and $\tan\delta_d = 0$.

The performance of a 16 cm high pyramidal absorber that is backed by a 1 mm thick iron plate is shown in Fig. 12 for three different cases. The first scenario is when the material has the same magnetic and electric properties $\varepsilon_r = \mu_r = 1.5$ and $\tan\delta_d = \tan\delta_m = 0.5$. The two other cases are for a non-magnetic dielectric material and a magnetic material with $\varepsilon_r = 1$ and $\tan\delta_d = 0$.

The results demonstrate that a material with dielectric- or magnetic-only properties offers similar performance and can be used while designing the absorber. However, employing a material that offers, simultaneously, both electrical and magnetic loss properties reduce the reflection coefficient appreciably. For the shown cases, the reduction in the reflection coefficient is greater than 15 dB for the majority of the frequency range involved.

7. Comparison with Other Published Papers

In order to further assess the results obtained with the help of the simulations, they are compared here with those obtained by the authors of other works. The general feature of the results obtained is the decrease of the reflection coefficient as the frequency of the incident wave changes. This trend was also observed in [2], [4], [6], and [9], especially at frequencies below 5 GHz.

Table 1 shows various performance parameters identified in previously published papers and compares them with the outcomes of this work. It can be seen that most of the previous research ([5], [6], [10], and [11]) ignored the effect of the loss tangent, despite its significant impact on the reflection coefficient, as was demonstrated in Fig. 6. However, the remaining references made in Tab. 1 took into consideration small ranges of the loss tangent, thus its effect was not demonstrated clearly.

Most of the former literature has considered agricultural residuals and other cheap materials with the objective of reducing the cost of absorbers and find use for the leftover materials. However, it failed to consider the impact of moisture, as excessive moisture can cause degradation of the materials used in absorbers, affecting the permittivity value and, consequently, the absorption value. In other words, the performance of absorbers based on these materials becomes unpredictable.

As the absorbers are used mainly to cover the walls of anechoic chambers in order to prevent reflections generated in certain regions of the test environment, their thickness is a crucial parameter. This parameter determines the volume of the material used and, consequently, the cost of the solution. In [2]–[4], [8] and [9], pyramids having a total thickness of 15 cm were used (along with their base) and achieved average reflection coefficients between –21 and –44 dB. This meant a reflection level/cm of thickness ratio of –1.4 to –3 dB/cm. The experiments described in [6], [11] employed a material thickness of 25 cm with a base of 5 cm, or an overall thickness of 30 cm, but achieved reflection levels of –30 dB and –25 dB, respectively, thus obtaining a ratio of –1 to –0.83 dB/cm. However, in the three examples investigated in this paper, materials with a thickness of 8 cm, 16 cm, and 24 cm were used, with a 5 cm thick base, and achieved an average reflection coefficient of –52.6 dB, –56.7 to –66.5 dB, or –2.5 dB/cm, –2.7 dB/cm, and –2.3 dB/cm, respectively.

The fourth design example, which used magnetic and dielectric properties of the absorber material, achieved an average reflection of –67 dB, which is equivalent to – 3.2 dB/cm. This shows that performance of the absorber is much better when the material is characterized by equal values of relative permittivity and permeability.

8. Conclusions

The choice of the appropriate absorber is influenced by the required level of reflection, the thickness of the absorber, and its weight and cost. Relative permittivity and permeability impact the initial reflection at the surface of the absorber, and it was demonstrated analytically and through computer simulations that lower permittivity or permeability result in lower reflection coefficients. Moreover, the reflection coefficient can be appreciably reduced if the absorber material has equal values of relative permittivity and permeability.

Tab. 1. Performance comparison of the results obtained with those of previous papers.

Ref.	Material	Dimensions [cm]	Frequency range [GHz]	ε_r	$\tan\delta$	S_{11} [dB]	dB/cm
[2]	Rubber tire dust and rice husk (75:25)	Base 5 × 5 × 2, pyramid's height 13	7 – 13	3.43	0.048	Average –32.51	–2.27
[2]	Rubber tire dust and rice husk (50:50)		7 – 13	2.67	0.076	Average –22.03	–1.47
[2]	Rubber tire dust and rice husk (25:75)		7 – 13	2.08	0.103	Average –21.54	–1.44
[3]	SCB		0.1 – 20	1.44	0.161	Average –44.39	–2.96
[4]	Rice husk		0 – 20	1.91	0.079	Average –31.93	–2.12
[4]	A mixture of rice husk and coal		0 – 20	2.50	0.086	Average –43.5	–2.9
[5]	Water hyacinth	Square pyramid shape 5 × 5 × 13	0 – 20	NA	NA	Lowest about –30 dB, highest about –10 dB	–2.3 –0.77
[6]	Polyurethane	Base 10 × 10 × 5, pyramid height 25	1 – 10	3.5	NA	Better absorption at higher frequencies: below –30 dB from 3 GHz	–1
[6]	Carbon		1 – 10	2.6	NA		–1
[6]	Polyurethane with carbon		1 – 10	3.5 and 2.6	NA		–1
[8]	Rice husk	Triangle base of height 2, pyramid height 13, side lengths 5.6 × 5	1 – 20	2.9	0.084	Average –41.142	–2.7
[8]	Rice husk	Equilateral triangle, base height 2, pyramid height 13, side length 5.25 (3 sides)	1 – 20	2.9	0.084	Average –39.878	–2.6
[8]	Rice husk	Square base, height 2, pyramid height 13, side length 5 (4 sides)	1 – 20	2.9	0.084	Average –39.423	–2.6
[9]	Banana leaves	Hexagonal pyramid, base thickness 2, pyramid height of 13	0.01 – 20		1.014	Average –35.3	–2.4
[9]	Rice husk		0.01 – 20	3.22	0.827	Average –39.70	–2.6
[9]	Rice sraw		0.01 – 20	3.10	0.956	Average –38.92	–2.6
[9]	Banana leaves	Truncated hexagonal pyramid, base thickness 2, pyramid height 13, with truncated miniature hexagon	0.01 – 20	2.49	1.014	Average –35.37	–2.4
[9]	Rice husk		0.01 – 20	3.22	0.827	Average –35.94	–2.4
[9]	Rice straw		0.01 – 20	3.1	0.956	Average –37.2	–2.5
[10]	Kenaf	20 × 20 × 2	1 – 12	2	NA	NA	NA
[10]	Coconut coir			2.6			
[11]	Carbon	Base 10 × 10 × 5, pyramid height 25, with a tip of 1 × 1	0.01 – 10	2.6	NA	Mostly below –25	–0.83
This work	Carbon	Base 10 × 10 × 5, pyramid height 16	1 – 10	2.5	0.5	Average –52.6	–2.5
		Base 10 × 10 × 5, pyramid height 16	1 – 10	1.5	0.5	Average –56.66	–2.7
		Base 10 × 10 × 5, pyramid height 24	1 – 10	2.5	0.5	Average –66.5	–2.3
	Carbon with iron back plate	Iron back plate 10 × 10 × 1 mm base 10 × 10 × 5, pyramid height 16	1 – 10	μ_r=1, ε_r=1.5	δ_m=0, δ_d=0.5	Average –56.9	–2.7
			1 – 10	μ_r=1.5, ε_r=1	δ_m=0.5, δ_d=0	Average –51	–2.4
			1 – 10	μ_r=1.5, ε_r=1.5	δ_m=0.5, δ_d=0.5	Average –67	–3.2

The loss tangent of the absorber material is an important factor as well. It was demonstrated in the course of the simulations that larger values of the loss tangent reduce reflection. The shape of the absorber also influences the reflection, as pyramidal absorbers offer a gradual introduction of the absorbing material into the air, and they provide a greater degree of design freedom.

The results of this investigation may help designers choose the proper parameters of the absorber material to achieve better performance. If the proper material is not naturally available, combinations of various materials may be used to achieve the desired parameters for the absorber.

References

[1] A.A. Abu Sanad *et al.*, "The Prospect of Using Hollow Pyramidal Microwave Absorbers for 5G Anechoic Chamber Applications: A Review", *Journal of Applied Physics*, vol. 136, art. no. 230701, 2024 (https://doi.org/10.1063/5.0244666).

[2] M.F. Bin Abd Malek *et al.*, "Rubber Tire Dust-rice Husk Pyramidal Microwave Absorber", *Progress In Electromagnetics Research*, vol. 117, pp. 449–477, 2011 (https://doi.org/10.2528/PIER11040801).

[3] L. Zahid *et al.*, "Development of Pyramidal Microwave Absorber Using Sugar Cane Bagasse (SCB)", *Progress In Electromagnetics Research*, vol. 137, pp. 687–702, 2013 (https://doi.org/10.2528/pier13012602).

[4] H. Kaur, G. Deep, and V. Chawla, "Enhanced Reflection Loss Performance of Square Based Pyramidal Microwave Absorber Using Rice Husk-coal", *Progress In Electromagnetics Research M*, vol. 43, pp. 165–173, 2015 (https://doi.org/10.2528/PIERM15072603).

[5] A. Nuan-on *et al.*, "Design and Fabrication of Microwave Absorbers Using Water Hyacinth", *Engineering Access*, vol. 3, pp. 7–10, 2017 (https://doi.org/10.14456/mijet.2017.2)).

[6] S.I. Orakwue and I.P. Onu, "Pyramidal Microwave Absorber Design for Anechoic Chamber in the Microwave Frequency Range of 1 GHz to 10 GHz", *European Journal of Engineering and Technology Research*, vol. 4, pp. 1–3, 2019 (https://doi.org/10.24018/ejers.2019.4.10.1409).

[7] H. Nornikman, P.J. Soh, A.A.H. Azremi, and M.S. Anuar, "Performance Simulation of Pyramidal and Wedge Microwave Absorbers", *2009 3rd Asia International Conference on Modelling and Simulation,* Bundang, Indonesia, 2009 (https://doi.org/10.1109/AMS.2009.13).

[8] H. Nornikman *et al.*, "Reflection Loss Performance of Triangular Microwave Absorber", *International Symposium on Antennas and Propagation*, 2010 [Online] Available: https://www.ieice.org/cs/isap/ISAP_Archives/2010/pdf/281.pdf.

[9] H. Nornikman, F. Malek, P.J. Soh, and A.A.H. Azremi, "Reflection Loss Performance of Hexagonal Base Pyramid Microwave Absorber Using Different Agricultural Waste Material", *2010 Loughborough Antennas and Propagation Conference, LAPC 2010*, Loughborough, UK, 2010 (https://doi.org/10.1109/LAPC.2010.5666029).

[10] L.M. Kasim *et al.*, "A Study of Electromagnetic Absorption Performance of Modern Biomass Wall Tile", *International Journal of Electrical and Electronic Engineering & Telecommunications*, vol. 9, pp. 429–433, 2020 (https://doi.org/10.18178/IJEETC.9.6.429-433).

[11] H. Nornikman, P.J. Soh, and A.A.H. Azremi, "Potential Types of Biomaterial Absorber for Microwave Signal Absorption", *4th International Conference on X Rays and Related Techniques in Research and Industries 2008 (ICXRI 2008)*, Kota Kinabalu, Sabah, Malaysia, 2008.

[12] Y.M. Zong, "Optimization of Multilayer Microwave Absorbers Using Multi-strategy Improved Gold Rush Optimizer", *ACES Journal*, vol. 39, pp. 708–717, 2024 (https://doi.org/10.13052/2024.ACES.J.390806).

[13] R. Xu *et al.*, "An Ultra-wideband Metamaterial Absorber with Angular Stability", *ACES Journal*, vol. 39, pp. 675–682, 2024 (https://doi.org/10.13052/2024.ACES.J.390802).

[14] M.B. Jasim and K. Sayidmarie, "Radar Cross-section Reduction of Planar Absorbers Using Resistive FSS Unit Cells", *Journal of Telecommunication and Information Technology*, no. 4, pp. 61–67, 2023 (https://doi.org/10.26636/jtit.2023.4.1331).

[15] M.F. Asmadi *et al.*, "The Optimal Performance of a Geopolymer Hollow Pyramidal Microwave Absorber with Triangular Slotted", *Solid State Phenomena*, vol. 344, pp. 97–102, 2023 (https://doi.org/10.4028/p-belmea).

[16] A.S. Yusof *et al.*, "Slotted Triangle on Hollow Pyramidal Microwave Absorber Characteristics", *2016 6th IEEE International Conference on Control System, Computing and Engineering (ICCSCE)*, Penang, Malaysia, 2016 (https://doi.org/10.1109/ICCSCE.2016.7893639).

[17] D.M. Pozar, *Microwave Engineering*, John Wiley & Sons, 3rd ed., 720 p., 2005 (ISBN: 9780471448785).

Aya Raad Thanoon, PG Student
Department of Communication Engineering
https://orcid.org/0009-0006-5000-4765
E-mail: ayah.dhunun2012@stu.uoninevah.edu.iq
Ninevah University, Mosul, Iraq
https://uoninevah.edu.iq/en/

Khalil H. Sayidmarie, Professor
Department of Communication Engineering
https://orcid.org/0000-0001-6525-0949
E-mail: kh.sayidmarie@uoninevah.edu.iq
Ninevah University, Mosul, Iraq
https://uoninevah.edu.iq/en/